ChemComm

Accepted Manuscript

This article can be cited before page numbers have been issued, to do this please use: S. Datta and S. Bhattacharya, *Chem. Commun.*, 2015, DOI: 10.1039/C5CC05367F.

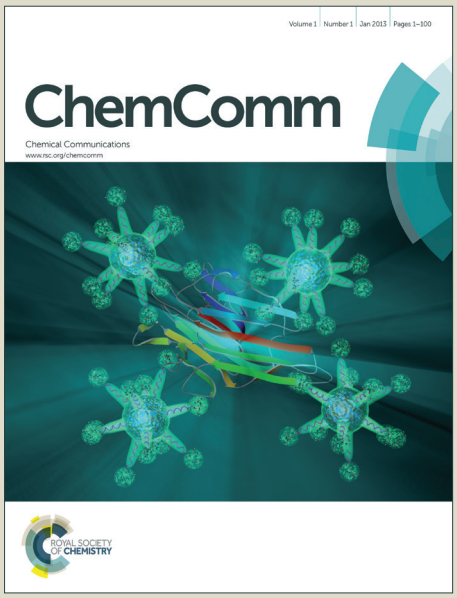

View Article Online
DOI: 10.1039/C5CC05367F

ChemComm

COMMUNICATION

Ag^+-induced reverse vesicle to helical fiber transformation in a self-assembly by tinkering around the keto-enol equilibrium of a chiral salicylideneaniline

Received 00th January 20xx,
Accepted 00th January 20xx

DOI: 10.1039/x0xx00000x

www.rsc.org/

Sougata Datta,[a] and Santanu Bhattacharya[*ab]

A new chiral amphiphilic salicylideneaniline bearing a terminal pyridine was synthesized. It formed reverse vesicles in toluene. Addition of Ag^+ to this however, reversibly transforms these reverse vesicles into left-handed nanohelices accompanied by spontaneous gel formation at room temperature.

Stimuli-responsive supramolecular systems[1] endowed with specific function have received considerable attention owing to their propensity to undergo specific structural transformation mediated by an external trigger.[2] These examples mimic natural phenomena like the seismonastic movement of mimosa leaves or tight curling up of millipedes upon touching.[1a] A wide range of low molecular-weight gelators (LMWGs)[3] has been examined either as nanomaterials[4] or biomaterials[5] due to their diverse nature of constitution and arrangements at the molecular level.[6] There are a few reports of stimuli- (*i.e.*, light,[7] mechanical,[8] redox,[9] charge-transfer[10] *etc.*) responsive sphere-to-fiber transformation accompanied by sol-to-gel transition. Yao demonstrated a reversible structural transition between nanofibers and normal vesicles from the self-assembly of a tripeptide-bipyridine conjugate.[8] There are also other examples of vesicle-to-fiber transformation that are devoid of sol-to-gel transition.[11] However, reverse vesicle-to-helical fiber transformation accompanied by sol-to-gel transition is still not known.

Salicylideneanilines and related compounds are interesting because of their intrinsic photochromic and/or thermochromic properties, as originated from the variation of population of the enol (–OH) and keto (–NH) forms due to their propensity to tautomerize.[12] Lu *et al*. reported a remarkable thermochromism from a salicylideneaniline organogelator.[12d] By following the equilibrium between the enol and keto forms, an evidence of thermochromism in a salicylideneaniline gel was established with the help of ^{1}H-NMR spectroscopy.[12c]

Aida[13a,b] and Lee[13c] independently reported Ag^+-induced supramolecular assembly by manipulation of non-covalent interactions at the molecular level. These observations prompted us to prepare a novel salicylideneaniline having a terminal pyridine and L-alanine based spacer (Figure 1a and Scheme S1, SI). This compound upon dispersion in toluene adopted a spherical morphology *via* self-assembly in the dispersed sol state due to the formation of reverse vesicles. This however, transformed reversibly into left-handed helical nanofibers through the transcription of molecular chirality into supramolecular helicity by selective supramolecular response of Ag^+ which was also accompanied by gel formation at room temperature.

The compound **1**, when dispersed in toluene, appeared as a nearly colourless suspension (Figure 1b). However, when an ethanolic or methanolic solution of $AgSO_3CF_3$ was added to **1** in toluene at a molar ratio of 1:2 [$(\mathbf{1})_2Ag^+$, ESI-MS: m/z 1129.64 ($C_{58}H_{84}AgN_8O_8)^+$], the viscosity of the resulting mixture gradually increased to form a robust yellow coloured gel (minimum gelator concentration [mgc] = 3.9 mM) quickly in 100/1 (v/v) toluene/ethanol. Whereas, the compound **2** containing a phenyl ring instead of the 3-pyridyl group did not furnish gel in the presence of Ag^+ (Figure 1a). It may be noted that the addition of an excess Ag^+ (>0.5 equiv.) led to the disruption of the gelation process. When an equal volume (1 ml) of an aq. solution of EDTA[14] (4 mM) was placed on the top of the gel, and gently stirred for 3 min, the gel transformed completely into a colourless sol. The mixture was allowed to settle for ~15 min until the aq. and organic layers phase separated. The stability constants of Ag^+-coordination complexes of pyridine and EDTA are 2 and 7.3 respectively.[14b] Therefore, Ag^+ could be removed from the organic phase by partitioning into the aq. solution of EDTA and the yellow gel could be reverted back to its previous colourless sol form again. The colourless toluene layer was taken out from the top of the aq. phase and could be induced to gelation again by addition of Ag^+ ion. The compound **1** however, did not respond to other metal ions, *e.g.,* Li^+, Cu^{2+}, Zn^{2+}, Co^{2+} and Cr^{3+} *etc.* Gelation was not observed also in the presence of *n*-$Bu_4N^+SO_3CF_3^-$. This excludes the role of triflate anion, which was only chosen to have adequate solubility of Ag^+ in an organic medium.

[a] Department of Organic Chemistry, Indian Institute of Science, Bangalore, India. Fax: +91-80-23600529; Tel: +91-80-22932664; E-mail: sb@orgchem.iisc.ernet.in
[b] Chemical Biology Unit, Jawaharlal Nehru Centre for Advanced Scientific Research, Bangalore, India
Electronic Supplementary Information (ESI) available. See
DOI: 10.1039/x0xx00000x

View Article Online
DOI: 10.1039/C5CC05367F

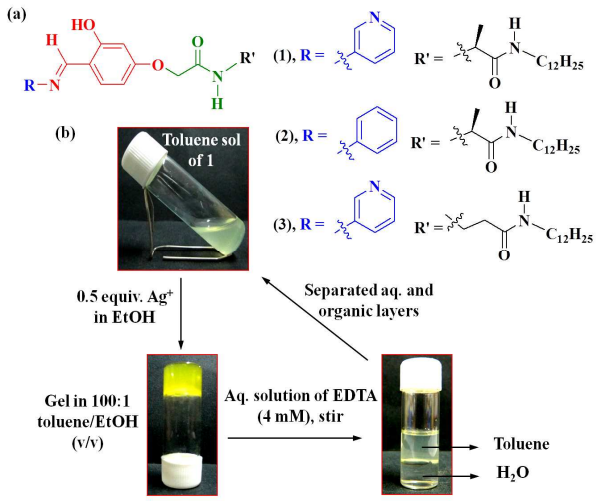

Fig. 1 (a) Molecular structures of the salicylideneanilines (**1-3**); (b) photographs showing Ag^+-mediated reversible sol-to-gel transition of **1** (3.9 mM) in toluene in presence of 1% EtOH (v/v).

In Raman spectra, the pyridyl ring of **1** in the breathing mode at 990 cm^{-1} shifted to 1020 cm^{-1} after its coordination with Ag^+ (Figure S24, SI). The band shift may be regarded as a sign of the pyridyl coordination of Ag^+.[15] The complexation of Ag^+ with **1** was also investigated using ^{1}H-NMR spectroscopy. With the addition of 0.5 equiv. of $AgSO_3CF_3$ in CD_3OD (1% v/v) to the [D_6]benzene solution of **1**, the *ortho*- and *meta*-protons of the pyridyl group of **1** shifted upfield, and that of the *para*-proton of the pyridyl group shifted downfield (Figure S25, SI).[15,16] As shown in Figure S26 (SI), a broad absorption band appeared in the range of 400-500 nm[12c-e] in the UV-Vis spectrum of Ag^+-complex of **1** in 100:1 (v/v) toluene/ethanol. This however, did not appear in the case of **1** alone, indicating the conversion to a higher population of keto form after Ag^+ complexation. CD-spectra of **1** in 100:1 (v/v) toluene/ethanol showed only one negative Cotton effect at 290 nm and a shoulder at 330 nm as a result of π-π* and *n*-π* transitions related to the π- and non-bonding electrons (Figure S27, SI).[17] However, a new negative peak near 400 nm associated with the salicylideneaniline chromophore appeared in the Ag^+-coordination complex, which suggests an anti-clockwise orientation of dipoles in the supramolecular aggregates. Figure S28 (SI) shows cyclic voltammetry plots of **1** and its Ag^+-complex in 5:1 (v/v) toluene/acetonitrile mixture in presence of 0.1 (M) *n*-$Bu_4N^+PF_6^-$ as a supporting electrolyte. Half-wave reduction potential of **1** associated with the pyridyl group appeared at -1.06 V which shifted to -0.87 V after complexation with Ag^+.

Scanning electron microscopy (SEM) of the toluene sol of **1** revealed the presence of spherical aggregates with diameters of 5-20 μm (Figure 2a). Morphology of **1** in toluene was further investigated by atomic force microscopy (AFM). The height images (Figure 2c and S29a, SI) obtained by tapping-mode on freshly cleaved mica sheets revealed the formation of nano- to micro-sized vesicle-like spherical aggregates (0.1-1 μm). In order to confirm the existence of reverse vesicles, a dye encapsulation experiment was performed by preparing a toluene dispersion of **1** (3.9 mM) in the presence of a hydrophobic dye, Nile red (0.39 mM).[18] Free dye could be removed by dialyzing the sample against toluene for ~72 h. When the dialyzed sample was examined under a fluoresence microscope, red-light emitting spherical aggregates (1-10 μm) were observed (Figure S30a, SI). This result clearly suggests the presence of an inner hydrophobic compartment inside these spherical aggregates (Figure S30b, SI). The hollow nature of the spherical assemblies (50-200 nm) was further evident from the difference in contrast between the periphery and the inner part of the nano-spheres in the TEM image (Figure S31a-b, SI).[8,18,19] Dynamic light scattering (DLS) experiment was performed to acquire information regarding the average hydrodynamic diameters of the reverse vesicles. Toluene sol of **1** afforded two types of aggregates of ~0.2 and ~2 μm (Figure S32, SI). This result is in good accordance with the different sizes observed under SEM, AFM and TEM experiments. The average size (z-average diameter) and the polydispersity index (PDI) of the reverse vesicles of **1** (0.39 mM) obtained from DLS experiment are 983.5 ± 0.7 nm and 0.429 ± 0.03 respectively.

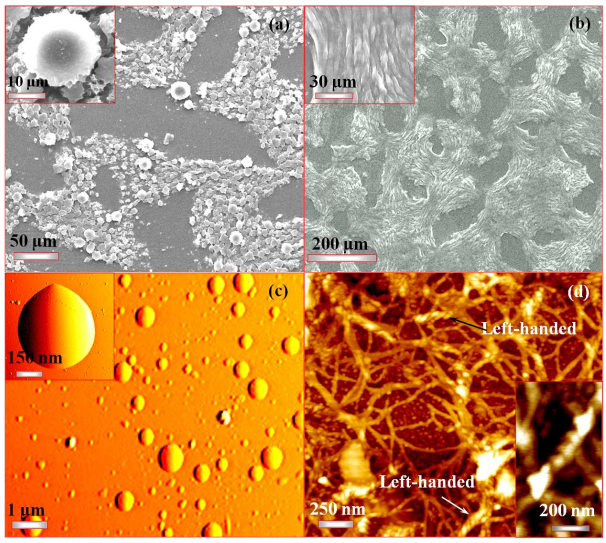

Fig. 2. (a and b) SEM and (c and d) AFM images of **1** and its Ag^+-coordination complex in 100:1 toluene/EtOH (v/v).

However, when the toluene gel formed upon Ag^+-coordination of **1** was examined under SEM, presence of fibrous networks (width 1-5 μm) was clearly observed (Figure 2b). Interestingly, AFM image of Ag^+-complex of **1** unveiled fibrous assemblies with entangled left-handed-helical architecture of high aspect ratio with widths of about 50-100 nm (Figure 2d and S29b, SI). Coexistence of reverse vesicles and helical nanofibers was found in case of intermediate stoichiometry of Ag^+ (0.25 equiv.) due to partial structural transformation (Figure 33a and 33b). Furthermore it is noteworthy that these helical nanofibers could be converted to reverse vesicles by the removal of Ag^+ upon treatment of an aq. solution of EDTA. The achiral analogue (**3**) of compound **1** (Figure 1a) containing β-alanine spacer instead of L-alanine also formed reverse vesicles (0.1-2 μm) in toluene (Figure S34a and S34c, SI). However, micro tape-like morphology was found in the xerogel of the corresponding Ag^+-coordination complex of compound **3** (Figure S34b and S34d, SI). This result clearly indicates that the formation of helical

View Article Online
DOI: 10.1039/C5CC05367F

nanofibers by Ag^+-coordination complex gel of **1** is attributed to the transcription of molecular chirality associated with the L-alanine spacer into supramolecular helicity.

Figure S35 (SI) shows ^{1}H-NMR spectra of the colourless sol of 3.9 mM **1** in [D_6]benzene in presence of CD_3OD (1% v/v). Two ^{1}H-NMR signals appear at δ = 12.5 and 13.5 respectively. These may be interpreted due to the existence of an equilibrium between the enol (–OH) and keto (–NH) forms. The peak that appears at δ = 13.5, is assigned to the -OH form because of the higher electronegativity of O than that of N.[12c] The peak associated with the enol form at δ = 13.5 is more intense and sharper compared to that of the keto form which appears at δ = 12.5. Thus the population of the colourless enol form is predominant in the toluene sol of **1**.[12c] Interestingly, the ^{1}H-NMR spectrum of the gel formed upon Ag^+ coordination of **1** (Ag^+:**1** = 1:2) shows a single peak at δ = 12.5 associated with the keto form and the signal at δ = 13.5 corresponding to the enol form disappears. This suggests that the keto form exists almost exclusively in the yellow gel phase. Consistent with the results of the ^{1}D-NMR experiment, two peaks at δ = 12.5 and 13.5 associated with the keto and enol forms respectively were observed along the diagonal of the H-H COSY spectrum of compound **1** in C_6D_6 (Figure S20, SI). In addition, a cross peak corresponding to the NH-H6 correlation associated with the keto form was observed. In contrast only a single peak along the diagonal at δ = 12.5 and a cross peak corresponding to the NH-H6 correlation associated with the keto form were observed in the H-H COSY spectrum of the Ag^+ coordination complex gel of **1** in C_6D_6 (Figure S23, SI). This result again confirms the exclusive existence of the keto form in the C_6D_6 gel phase while the enol form is predominant in the sol state in C_6D_6. It is also important to note that a single peak at δ = 13.2 associated with the enol form of **1** was observed in the NMR-spectra in $CDCl_3$ indicating the sole existence of the enol form in the $CDCl_3$ solution presumably because of the lack of aggregation of **1** in this medium (Figure S1 and S16, SI). According to Ogawa and Arai,[20] the energy differences between the ground states of the -OH and -NH forms in solution may be too large to allow conversion of the enol to keto form. However, Lu's group and us independently established that the -NH form could be stabilized in the aggregates of the gel phase.[12c,d] This may significantly lower the energy barrier between the -OH and -NH forms than that in solution, which may in turn favour the proton tautomerization leading to the formation of the -NH form (Figure S36, SI). Interestingly, the ^{1}H-NMR spectrum of the residue obtained by evaporating the toluene layer after partitioning with the aq. solution of EDTA (4 mM) is identical to that of **1**, elucidating the reversibility of this transformation (Figure S35, SI). This result clearly explains the colourless nature of the toluene sol and yellow colour of the Ag^+-coordinated gel.

Since the solution of **1** in $CHCl_3$ did not exhibit spherical nanostructures, we compared the ^{1}H-NMR spectrum of **1** in $CDCl_3$ with that in C_6D_6. The OH proton at δ = 13.5 in the ^{1}H-NMR spectrum of **1** in [D_6]benzene shifted to δ = 13.2 in $CDCl_3$ (Figure S37, SI). Similarly, the pyridyl protons shifted upfield as the solvent was changed from C_6D_6 to $CDCl_3$ (Figure S37, SI). These results illustrate the existence of intermolecular H-bonding between the N-atom of the pyridyl group and the hydrogen atom of the *ortho*-hydroxy group (Figure 3). This was further supported from the 2D-NMR experiment. In the H-H NOESY spectrum of compound **1** in $CDCl_3$, a cross peak was observed as associated with the H3-H6 correlation (Figure S17, SI). This result indicates that the pyridyl N atom remains in the same side of the OH group of the salicylidene ring (Figure S38, SI). While, the H1-H6 correlation was observed in the H-H NOESY spectrum (Figure S21, SI) of the compound **1** in C_6D_6 indicating an anti-arrangement between the pyridyl N atom and the OH group of the salicylidene ring (Figure S38, SI). This arrangement is favourable for the inter-molecular H-bonding between the N-atom of the pyridyl group and the hydrogen atom of the *ortho*-hydroxy group to give rise to a lamellar organization which finally leads to the formation of reverse vesicles in C_6D_6 (Figure 3).

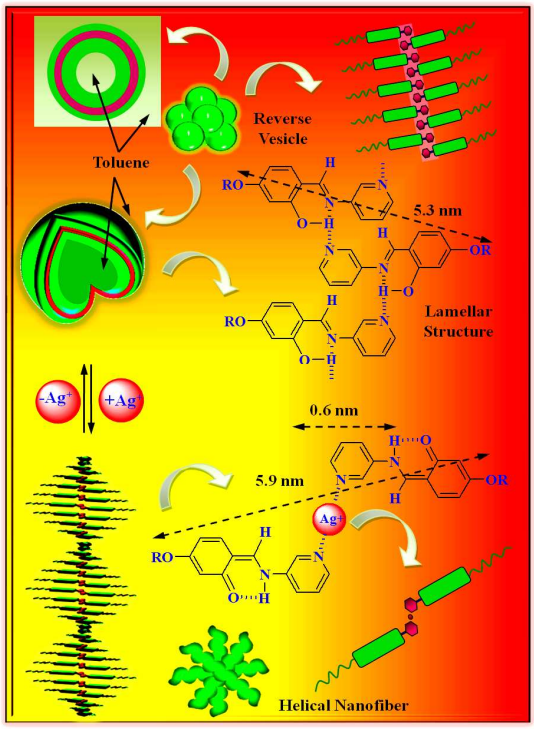

Fig. 3 Molecular packing model and a schematic representation of Ag^+-induced reverse vesicle to nanohelix transformation.

Prevalence of inter-molecular H-bonding interactions among the amide linkages of Ag^+-coordination complex of **1** in the gel phase has been further evidenced from the solvent and concentration-dependent FTIR-spectroscopy (Figure S39, SI). The small-angle X-ray diffraction pattern of **1** in toluene (Figure S40a, SI) corresponds to a lamellar arrangement.[12c-e,21] In the low-angle range (2θ ~1-12°), six peaks with *d*-spacings of 5.3, 2.65, 1.76, 1.32, 1.06 and 0.88 nm were observed with *d*-spacing ratios of 1:1/2:1/3:1/4:1/5:1/6 respectively. This is the characteristic of a lamellar structure with a domain spacing of 5.3 nm, a value less than the double of its molecular length, 5.8 nm as calculated from the geometry optimization of one molecule of **1** using B3LYP/6-31G* (Figure S41, SI). This analysis once again suggests that the pyridyl heads presumably interdigitate with each other to facilitate intermolecular H-bonding interactions between the N-atom of the pyridyl group and the H-atom of the *ortho*-hydroxy group. In contrast, the longest repeat distance shifts from 5.3 to 5.9 nm in

View Article Online
DOI: 10.1039/C5CC05367F

the Ag^+-coordination complex of **1** (Ag^+:**1** = 1:2), a fact that is clearly consistent with the proposed model of the structural transformation (Figure 3 and S40b, SI).

In conclusion, we have demonstrated a self-assembly of a pyridine appended chiral salicylideneaniline, **1**, that forms reverse vesicles in toluene by adopting a lamellar organization. Interestingly, the colourless reverse vesicles transform into helical organizations reversibly on addition of Ag^+ accompanied by a yellow coloured gel formation. This is the first report where a reverse vesicle-to-helical structural transformation accompanied by sol-to-gel transition takes place as confirmed by both microscopy and X-ray diffraction analysis. The formation of reverse vesicles was further evidenced from a dye entrapment study. Therefore, this type of structural transformation may be useful in achieving a stimuli-driven delivery. Thus a keto-enol-tautomerism associated with the gel-to-sol transition has been demonstrated unambiguously using visible colour change, UV-Vis absorption and ^{1}H-NMR spectral studies. It has been also possible to confirm the presence of the keto form exclusively in the gel phase by recognizing a distinguishable ^{1}H-NMR signal. It is may be further emphasized that examples of reverse vesicles are scarce compared to the aggregates formed in aq. media (normal micelles or vesicles). Whenever such reports of reverse micelles or vesicles are known they are generally observed from lipids and polymers *etc*.[18a,22] Accordingly the formation of reverse vesicles from such a simple salicylideneaniline is indeed unprecedented and may spur new research activity.

This work was supported by J. C. Bose fellowship of DST to S.B. S.D. thanks CSIR for a senior research fellowship.

Notes and references

1 (a) S. Datta and S. Bhattacharya, *Chem. Soc. Rev.*, 2015, DOI: 10.1039/c5cs00093a; (b) A. C. Coleman, J. M. Beierle, M. C. A. Stuart, B. Maciá, G. Caroli, J. T. Mika, D. J. van Dijken, J. Chen, W. R. Browne and B. L. Feringa, *Nat. Nanotechnol.*, 2011, **6**, 547; (c) L. Zhang, L. Qin, X. Wang, H. Cao and M. Liu, *Adv. Mater.*, 2014, **26**, 6959; (d) H. Cao, X. Zhu and M. Liu, *Angew. Chem., Int. Ed.*, 2013, **52**, 4122; (e) K. Dan and S. Ghosh, *Angew. Chem., Int. Ed.*, 2013, **52**, 7300; (f) Z. Zhang, C. Zhan, X. Zhang, S. Zhang, J. Huang, A. D. Q. Li and J. Yao, *Chem. Eur. J.*, 2012, **18**, 12305; (g) D. Ke, C. Zhan, S. Xu, X. Ding, A. Peng, J. Sun, S. He, A. D. Q. Li and J. Yao, *J. Am. Chem. Soc.*, 2011, **133**, 11022.

2 (a) K. R. Raghupathi, U. Sridhar, K. Byrne, K. Raghupathi and S. Thayumanavan, *J. Am. Chem. Soc.*, 2015, **137**, 5308; (b) Z. Shen, T. Wang, L. Shi, Z. Tang and M. Liu, *Chem. Sci.*, 2015, **6**, 4267; (c) M. D. Segarra-Maset, V. J. Nebot, J. F. Miravet and B. Escuder, *Chem. Soc. Rev.*, 2013, **42**, 7086; (d) S. Datta, S. K. Samanta and S. Bhattacharya, *Chem. Eur. J.*, 2013, **19**, 11364; (e) X. Yang, G. Zhang and D. Zhang, *J. Mater. Chem.*, 2012, **22**, 38; (f) C. Wang, Q. Chen, F. Sun, D. Zhang, G. Zhang, Y. Huang, R. Zhao and D. Zhu, *J. Am. Chem. Soc.*, 2010, **132**, 3092; (g) P. K. Vemula, J. Li and G. John, *J. Am. Chem. Soc.*, 2006, **128**, 8932.

3 (a) S. Datta and S. Bhattacharya, *Soft Matter*, 2015, **11**, 1945; (b) P. Xue, B. Yao, J. Sun, Z. Zhang and R. Lu, *Chem.Commun.*, 2014, **50**, 10284; (c) K. K. Kartha, S. S. Babu, S. Srinivasan and A. Ajayaghosh, *J. Am. Chem. Soc.*, 2012, **134**, 4834; (d) S. R. Jadhav, P. K. Vemula, R. Kumar, S. R. Raghavan and G. John, *Angew. Chem., Int. Ed.*, 2010, **49**, 7695.

4 (a) J. Nanda, A. Biswas, B. Adhikari and A. Banerjee, *Angew. Chem., Int. Ed.*, 2013, **52**, 1; (b) S. Bhattacharya, A. Srivastava and A. Pal, *Angew. Chem., Int. Ed.*, 2006, **45**, 2934.

5 (a) P. K. Vemula and G. John, *Acc. Chem. Res.*, 2008, **41**, 769; (b) A. R. Hirst, B. Escuder, J. F. Miravet and D. K. Smith, *Angew. Chem., Int. Ed.*, 2008, **47**, 8002.

6 (a) J. H. Jung, J. H. Lee, J. R. Silverman and G. John, *Chem. Soc. Rev.*, 2013, **42**, 924; (b) T. Tu, W. Fang, X. Bao, X. Li and K. H. Dötz, *Angew. Chem. Int. Ed.*, 2011, **50**, 6601; (c) J. A. Foster and J. W. Steed, *Angew. Chem., Int. Ed.*, 2010, **49**, 6718; (d) M.-O. M. Piepenbrock, G. O. Lloyd, N. Clarke and J. W. Steed, *Chem. Rev.*, 2010, **110**, 1960; (e) P. Dastidar, *Chem. Soc. Rev.*, 2008, **37**, 2699. (f) D. J. Abdallah and R. G. Weiss, *Adv. Mater.*, 2000, **12**, 1237; (g) P. Terech and R. G. Weiss, *Chem. Rev.*, 1997, **97**, 3133.

7 G. John, G. Zhu, J. Li and J. S. Dordick, *Angew. Chem., Int. Ed.*, 2006, **45**, 4772.

8 D. Ke, C. Zhan, A. D. Q. Li and J. Yao, *Angew. Chem., Int. Ed.*, 2011, **50**, 3715.

9 X. Miao, W. Cao, W. Zheng, J. Wang, X. Zhang, J. Gao, C. Yang, D. Kong, H. Xu, L. Wang and Z. Yang, *Angew. Chem., Int. Ed.*, 2013, **52**, 7781.

10 M. R. Molla and S. Ghosh, *Chem. Eur. J.*, 2012, **18**, 9860.

11 (a) Q. Yan and Y. Zhao, *Angew. Chem., Int. Ed.*, 2013, **52**, 9948; (b) Y. Yan, H. Wang, B. Li, G. Hou, Z. Yin, L. Wu and V. W. W. Yam, *Angew. Chem., Int. Ed.*, 2010, **49**, 9233; (c) J.-H. Ryu, E. Lee, Y.-b. Lim and M. Lee, *J. Am. Chem. Soc.*, 2007, **129**, 4808; (d) A. Ajayaghosh, P. Chithra and R. Varghese, *Angew. Chem. Int. Ed.*, 2007, **46**, 230; (e) J.-H. Ryu, H.-J. Kim, Z. Huang, E. Lee and M. Lee, *Angew. Chem., Int. Ed.*, 2006, **45**, 5304; (f) C. Park, I. H. Lee, S. Lee, Y. Song, M. Rhue and C. Kim, *Proc. Natl. Acad. Sci. USA*, 2006, **99**, 5355.

12 (a) K. Fan, J. Yang, X. Wang and J. Song, *Soft Matter*, 2014, **10**, 8370; (b) K. Fan, J. Song, J. Li, X. Guan, N. Tao, C. Tong, H. Shen and L. Niu, *J. Mater. Chem. C*, 2013, **1**, 7479; (c) S. Datta and S. Bhattacharya, *Chem. Commun.*, 2012, **48**, 877; (d) P. Chen, R. Lu, P. Xue, T. Xu, G. Chen and Y. Zhao, *Langmuir*, 2009, **25**, 8395; (e) P. Xue, R. Lu, G. Chen, Y. Zhang, H. Nomoto, M. Takafuji and H. Ihara, *Chem. Eur. J.*, 2007, **13**, 8231.

13 (a) T. Fukino, H. Joo, Y. Hisada, M. Obana, H. Yamagishi, T. Hikima, M. Takata, N. Fujita and T. Aida, *Science*, 2014, **344**, 499; (b) A. Kishimura, T. Yamashita and T. Aida, *J. Am. Chem. Soc.*; 2005, **127**, 179; (c) H.-J. Kim, J.-H. Lee and M. Lee, *Angew. Chem., Int. Ed.*, 2005, **44**, 5810.

14 (a) W. Fang, C. Liu, Z. Lu, Z. Sun and T. Tu, *Chem. Commun.*, 2014, **50**, 10118; (b) W. Hong, W. Li, X. Hu, B. Zhao, F. Zhang and D. Zhang, *J. Mater. Chem.*, 2011, **21**, 17193.

15 Q. Liu, Y. Wang, W. Li and L. Wu, *Langmuir*, 2007, **23**, 8217.

16 K. Chen, L. Tang, Y. Xia and Y. Wang, *Langmuir*, 2008, **24**, 13838.

17 C. H. Sung, L. R. Kung, C. S. Hsu, T. F. Lin and R. M. Ho, *Chem. Mater.*, 2006, **18**, 352.

18 (a) A. Das and S. Ghosh, *Macromolecules*, 2013, **46**, 3939; (b) X. Zhang, S. Rehm, M. M. Safont-Sempere and F. Würthner, *Nat. Chem.*, 2009, **1**, 623.

19 (a) J. Zhang, Y.-F. Song, L. Cronin and T. Liu, *Chem. Eur. J.*, 2010, **16**, 11320; (b) X.-N. Xu, L. Wang and Z.-T. Li, *Chem. Commun.*, 2009, 6634.

20 (a) A. Ohshima, A. Momotake and T. J. Arai, *Photochem. Photobiol. A*, 2004, **162**, 473; (b) K. Ogawa and J. Harada, *J. Mol. Struct.*, 2003, **647**, 211; (c) K. Ogawa, Y. Kasahara, Y. Ohtani and J. Harada, *J. Am. Chem. Soc.*, 1998, **120**, 7107.

21 M. George, S. L. Snyder, P. Terech, C. J. Glinka and R. G. Weiss, *J. Am. Chem. Soc.*, 2003, **125**, 10275.

22 (a) H.-Y. Lee, K. K. Diehn, K. Sun, T. Chen and S. R. Raghavan, *J. Am. Chem. Soc.*, 2011, **133**, 8461; (b) S-H. Tung, H.-Y. Lee and S. R. Raghavan, *J. Am. Chem. Soc.*, 2008, **130**, 8813. (c) D. Domínguez-Gutiérrez, M. Surtchev, E. Eiser and C. J. Elsevier, *Nano Lett.*, 2006, **6**, 145; (d) A. Ajayaghosh, R. Varghese, S. Mahesh and V. K. Praveen, *Angew. Chem., Int. Ed.*, 2006, **45**, 7729; (e) S. Basu, D. R. Vutukuri, S. Thayumanavan, *J. Am. Chem. Soc.*, 2005, **127**, 16794. (f) S. Basu, D. R. Vutukuri, S. Shyamroy, B. S. Sandanaraj and S. Thayumanavan, *J. Am. Chem. Soc.*, 2004, **126**, 9890.